ELSEVIER

Journal of Molecular Catalysis A: Chemical 137 (1999) 273–286

JOURNAL OF MOLECULAR CATALYSIS A: CHEMICAL

Selective catalytic reduction of NO with hydrocarbon on Cu^{2+}-exchanged pillared clay: An IR study of the NO decomposition mechanism

Mala Sirilumpen, Ralph T. Yang *, Nopparat Tharapiwattananon

Department of Chemical Engineering, University of Michigan, Ann Arbor, MI 48109-2136, USA

Received 25 June 1997; accepted 11 March 1998

Abstract

In an earlier study, it has been found that Cu^{2+} ion-exchanged pillared clay (Cu-PILC) has a substantially higher activity for the selective catalytic reduction of NO by ethylene over Cu-ZSM-5. Moreover, it is not significantly deactivated by water vapor and SO_2. In this study, the activity for direct NO decomposition in the presence of O_2 on Cu-PILC was studied and an in situ IR study for the key intermediates and the reaction mechanism was made. The direct NO decomposition activities for Cu-PILC and Cu-ZSM-5 were similar. Under in situ NO and O_2 reaction conditions at temperatures up to 300°C, IR absorption bands at well-defined peak positions are identified. The band at 1699 cm^{-1} is assigned to a dinitrosyl species on Cu^{+}. The bands with peaks at 1609, 1530–1480 and in the region of 1440–1335 cm^{-1} are assigned to bidentate nitrate, monodentate nitrate and nitro species bonded to Cu^{2+}. A redox mechanism is proposed for NO decomposition. The limiting step is thought to be the N–N coupling between surface nitrate and gaseous nitric oxide to form nitrogen. The existence of substantial amounts of nitrate formed from NO alone indicates the important role of the large amount of lattice oxygen that is available on Cu-PILC. As a result, the role of external oxygen supply is only to replenish the consumed lattice oxygen. The proposed NO decomposition mechanism suggests that the redox property of Cu-PILC is crucial for this reaction.

Keywords: NO reduction; Cu^{2+}-exchanged pillared clay; NO decomposition mechanism

1. Introduction

NO_x catalytic decomposition and reduction have been studied extensively because it is a major concern in air pollution. High NO_x emitted to the atmosphere from combustion sources contributes to acid rain and smog formation. More stringent regulations have been imposed recently to lower the pollutant emission of hydrocarbon, carbon oxides, nitric oxides and particulates. All of these pollutants excluding NO_x can be minimized by operating combustion engines at a high air to fuel ratio, i.e., under lean burn conditions [1]. Such highly oxidizing conditions would dramatically

* Corresponding author.

1381-1169/99/$ - see front matter
PII: S1381-1169(98)00112-5

diminish the activity of the catalyst used in conventional three way catalytic converters which are used to eliminate HC, CO, and NO_x. The situation becomes worse when the combustion temperature has been raised for higher standards of fuel efficiency [2–5]. These changes present a challenge to search for new catalysts or methods to deal with the increased NO concentrations from the lean-burn engines. Thus, many studies have been conducted to search for the best catalysts and alternate approaches which could selectively convert NO_x to nontoxic substances under the real exhaust conditions and compositions. Earlier research was focused on NO_x decomposition over noble metal catalysts [6]. This method is preferred because no additional chemicals are required to decompose NO_x to N_2 and O_2. Although direct decomposition is thermodynamically favorable, the rates are prohibitively low [7]. The first catalysts found to be active for selective catalytic reduction (SCR) of NO by hydrocarbons in the presence of oxygen were Cu^{2+} ion-exchanged ZSM-5 and other zeolites, reported in 1990 by Iwamoto [8] and Held et al. [9] and in early patents cited in [10]. Reports on a large number of catalysts for this reaction have appeared since 1990 [11,12]. The majority of these catalysts are ion-exchanged zeolites, including H^+ forms. Alumina and metal oxides supported on alumina have also been studied, but are less active. The early (1992–1993) literature on the subject, primarily by Japanese researchers, has been reviewed by Iwamoto and Mizuno [4] and will not be repeated here. The most active catalysts include: Cu-ZSM-5 [7–9,13–19], Co-ZSM-5 and Co-Ferrierite [18,20–22], Ce-ZSM-5 [10,23], and Cu–Zr–O and Cu–Ga–O [24,25]. Although Cu-ZSM-5 is the most active catalyst, it suffers from severe deactivation in engine tests, presumably due to H_2O and SO_2 [26–28]. Comprehensive reviews and discussion on the reaction were made recently by Amiridis et al. [12] and by Shelef [29]. More recently, Yang and Li [30] found that Cu^{2+} ion-exchanged pillared clay (PILC) has superior NO SCR activities (using C_2H_4). Based on the comparison of first-order rate constants between Cu^{2+}-PILC and Cu^{2+}-ZSM-5, the PILC catalyst was four times more active at 300°C, and more importantly, the PILC catalyst maintained high activities in the presence of H_2O and SO_2 [30]. The mechanism of the SCR reaction on Cu^{2+}-PILC is not understood [31].

This study was designed to obtain an understanding of NO decomposition on Cu^{2+}-PILC as the first step to understanding the SCR mechanism. Due to the similarity between Cu^{2+}-PILC and Cu-ZSM-5, the previously proposed mechanisms on Cu-ZSM-5 would provide some insights into the reaction on Cu^{2+}-PILC. For example, Li, Hall and Valyon have suggested that ''the working catalysts probably consist of a relatively small number of Cu(I) centers (or adjacent Cu(I) pairs) maintained in a steady state by balance of the rate of oxidation with the rate of O_2 desorption'' [32,33]. This is consistent with Iwamoto and Hamada [34] who studied the copper oxidation state and examined its influence on the interactions of Cu with adsorbates under various conditions by FTIR, ESR, TPR and other techniques. Giamello et al. also explained the redox cycle by N_2O elimination from the dinitrosyl species [35]. It has been suggested that N_2O_3 was an intermediate species [36,37]. Therefore, the main purpose of this study was to explore the NO decomposition mechanism by using mainly FTIR to study the surface species on Cu^{2+}-PILC under in situ conditions.

2. Experimental

2.1. Cu^{2+}-ion exchange and catalyst preparation

A delaminated form of pillared clay, delaminated Al_2O_3-pillared laponite, was used in this study. The PILC was prepared by Laporte Industries. The samples were pretreated by first suspending as 1%

slurry (by weight) and then washing with dilute NH_4NO_3 solution to remove impurities and remaining metal ions. After filtration, the residue was dried at 110°C in air and resuspended as 1% slurry (by wt.). 10 ml. of 0.1 M $Cu(NO_3)_2$ solution was added to 100 ml. slurry with constant stirring. The acidity of the solution was controlled to pH = 5.5 by using ammonium hydroxide and nitric acid solutions. The mixture was then kept at 50°C for 6 hire. The residue was then thoroughly washed 5 times with de-ionized water. After filtration, the solid sample was dried at 100°C for 24 h, crushed, sieved for the size fraction 80–100 US mesh and calcined at 400°C in air for 12 h. The amount of Cu^{2+} in the PILC was determined by atomic absorption spectroscopy. The catalyst contained 3.9% (by wt.) Cu, which corresponded to 87.7% ion exchange. From BET analysis, the sample surface areas were 384 $m^2\,g^{-1}$ and 318 $m^2\,g^{-1}$, respectively, for delaminated alumina-pillared laponite and its Cu^{2+}-exchanged form. A ZSM-5 with $Si/Al = 40$ was used in this work. The laponite was a synthetic hectorite, with a chemical analysis: $Na_{0.4}\ Mg_{5.6}\ Li_{0.4}\ Si_{8.0}\ O_{20}(OH)_4$.

2.2. FTIR spectroscopy

A Nicolet-400 spectrometer was used to record the FTIR spectra. Sample pressed into self-supporting wafers and mounted in a pyrex glass IR cell fitted with CaF_2 windows. The FTIR cell was

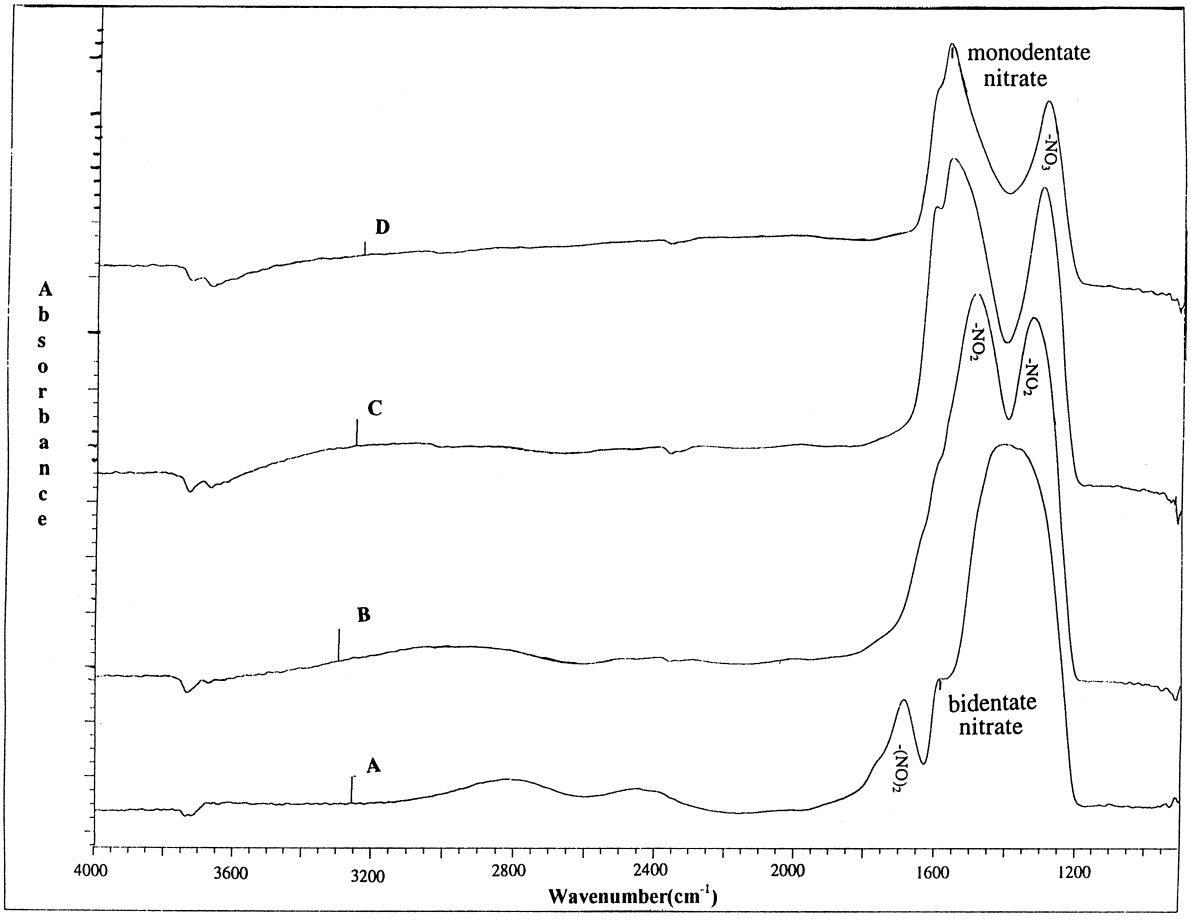

Fig. 1. Spectra of adsorbed species on Cu-PILC after NO (6000 ppm) adsorption for 0.5 h at 25°C and followed by He purge at 25°C (A), 100°C (B), 200°C (C) and 300°C (D).

designed for in situ reaction. A heating element cage surrounding a movable sample holder was employed to heat the catalyst temperature up to 450°C. The temperature was measured with a chromel–alumel thermocouple mounted close to the catalyst surface. Spectra were taken by accumulating 100 scans at a spectral resolution of 4 cm^{-1}. The focused wavelength range was 3000–900 cm^{-1} to observe the related nitro, nitrile, nitrito and nitrate species. A delaminated Cu^{2+}–Al_2O_3-pillared laponite wafer of about 25 $mg\,cm^{-2}$ was used for this study.

Before recording the background or sample spectra, the pellet was pretreated in a flow of He (ultrahigh purity grade) at 400°C for 2 h at a flow rate of 100 $ml\,min^{-1}$. After pretreatment, the background spectrum was recorded after the clean pellet remained at the desired temperature for 15 min to ensure thermal equilibrium. The background spectra were collected at several temperatures that corresponded to the in situ reaction temperatures. Subsequently, the catalyst was exposed to a stream of NO (0.6%) in He (supplied by Matheson Company, used without further purification) at a total flow rate of 60 $ml\,min^{-1}$ at room temperature for half an hour. Then, the gases were switched off and the catalyst was purged by He until there was no gas phase species shown in the spectrum. The sample was heated to the desired temperature at 10°C per min. Spectra were recorded sequentially from room temperature to 300°C at 100°C intervals. In addition, the effects of O_2 were also studied.

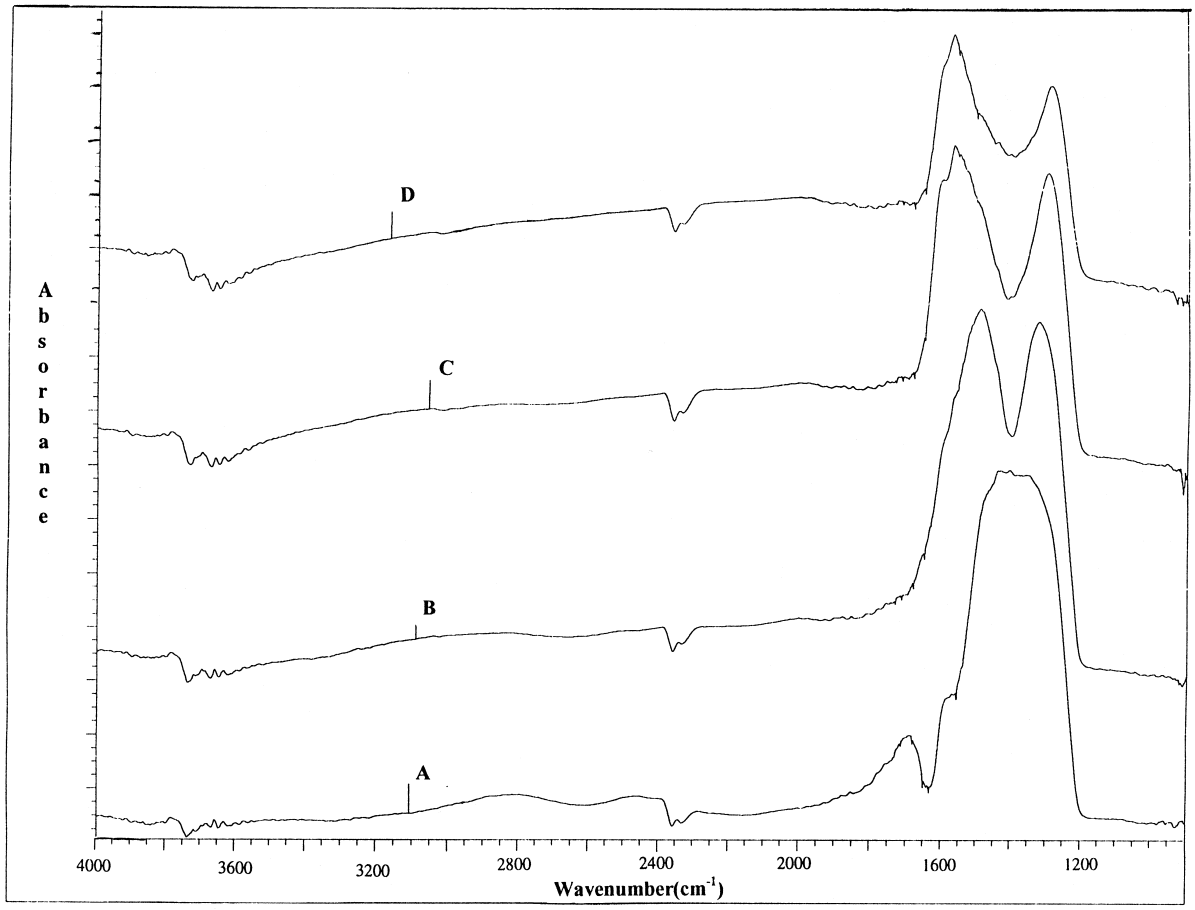

Fig. 2. Spectra of adsorbed species on Cu-PILC after NO (6000 ppm) and O_2 (2%) adsorption for 0.5 h at 25°C and followed by He purge at 25°C (A), 100°C (B), 200°C (C) and 300°C (D).

After the foregoing pretreatment, O_2 gas (99% purity) was mixed with the stream of NO (0.6%) in He by maintaining the total flow rate at 60 ml min^{-1}. The spectra were taken in two separate sets. One was for room temperature adsorption followed by He purge. The procedure for recording the spectra was the same as stated above for NO, performed from room temperature to 300°C. The other was to observe the difference by using a subtraction method under in situ conditions as to be described. The background was recorded in the reactant gases and then subtracted from the spectra of adsorbed species under those reactant gases at the same concentration for each temperature (i.e., 25, 100, 200 and 300°C).

2.3. NO decomposition and product analysis

Catalyst activity was studied in a fixed bed quartz micro reactor. The catalyst was subjected to pretreatment in a flow of He (ultrahigh purity) at 100 ml min^{-1} at 300°C for 2 h. The gas flow rates were regulated by volumetric flow controllers. A feed containing 10,000 ppm NO (in He) passed through 1 g sample supported on a quartz frit. The total gas flow was 15 cm^3 min^{-1}. The product

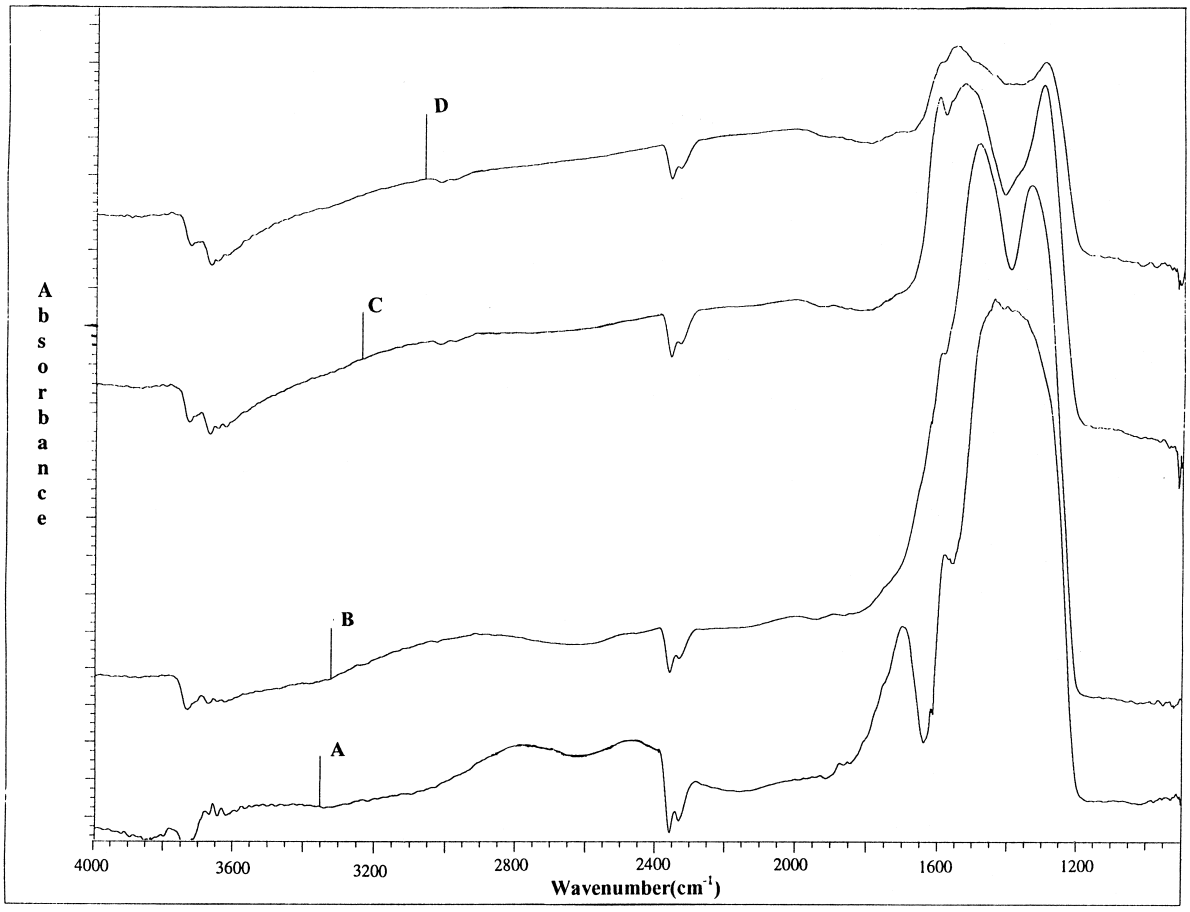

Fig. 3. Spectra of adsorbed species on Cu-PILC under NO (6000 ppm) and O_2 (2%), without He purge, at 25°C (A), 100°C (B), 200°C (C) and 300°C (D). The spectra were obtained by subtracting spectra without sample pellet from that with sample pellet, at the same temperatures.

stream was analyzed by a chemiluminescent NO/NO_x analyzer (Thermo Electron, Model 10), a mass spectrometer (UTI Instrument, model 100) and a gas chromatograph. The chemiluminescent NO/NO_x analyzer with a sensitivity of 1 ppm was used for continuous monitoring of the product NO concentration. The details of the reactor was given elsewhere [30,38]. For the mass spectrometric analysis, a quadrupole gas analyzer was used for N_2O analysis. In addition, a Shimadzu GC model 14A gas chromatograph was used to analyze the concentrations of N_2 and N_2O in the reaction product stream. A Poropak Q column was used to analyze N_2O and a molecular sieve 5A column to analyze N_2, O_2 and NO [39]. The temperature of the TCD detector was set at 25°C for both columns.

3. Results

3.1. In situ FTIR spectra of adsorbed species

Fig. 1 shows the FTIR spectra at various temperatures after 6000 ppm NO adsorption at room temperature on Cu^{2+}-Al-PILC. The IR absorption bands of gaseous NO are at 1900 and 1840 cm^{-1}.

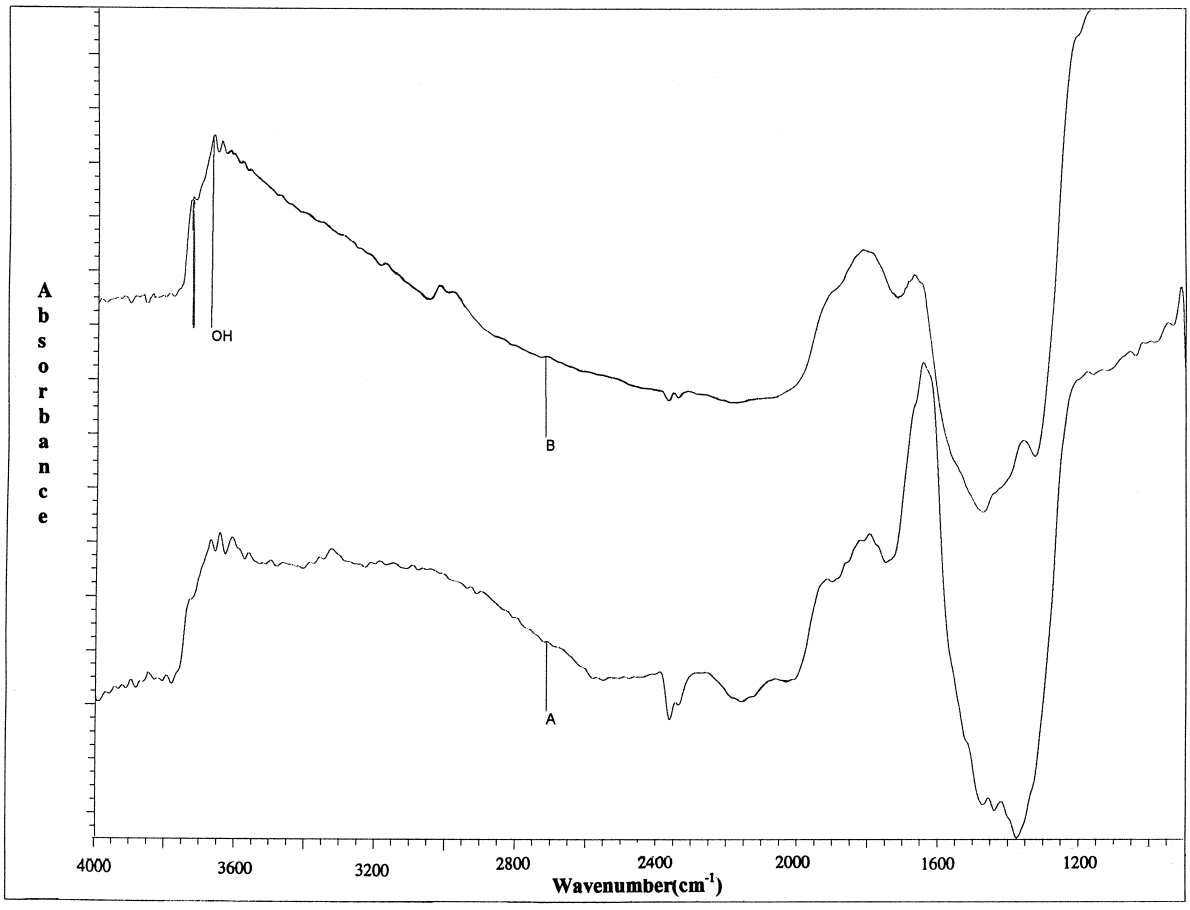

Fig. 4. Spectra of clean Cu-PILC showing O–H stretching frequencies (including hydrogen bonded, adsorbed water at 3000–3500 cm^{-1} and free surface hydroxyl groups at 3650–3750 cm^{-1}), taken at 25°C (A) and 300°C (B).

These two peaks vanished after purging with He for a short period. The remaining peaks appeared at 1699 cm^{-1}, 1603 cm^{-1} and a region of 1453–1310 cm^{-1}. Upon heating to 100°C, the substantial peak in the vicinity of 1450–1300 cm^{-1} resolved into two peaks, centered at 1493 and 1334 cm^{-1} while there was no noticeable intensity reduction. In contrast, the intensity of the small shoulder at 1603 cm^{-1} diminished somewhat while the band at 1699 cm^{-1} disappeared completely. Upon further increasing the temperature to 200°C, the pair of peaks at 1493 and 1334 cm^{-1} shifted slightly to higher and lower frequencies at 1571 and 1306 cm^{-1}. These two peaks demonstrated thermal stability up to 200°C and started decreasing their intensities when the temperature was increased to 300°C. A set of negative O–H stretching bands was also observed in the region of 3800–3600 cm^{-1} and gradually increased at higher temperatures.

Fig. 2 shows the FTIR spectra of Cu^{2+}-Al-PILC heat-treated to various temperatures after equilibrium with 6000 ppm NO and 2% O_2 at room temperature, followed by He purge. It clearly shows that the presence of O_2 did not form any additional species when compared to NO adsorption without O_2. All peaks were at the same positions as in Fig. 1.

Fig. 3 shows the FTIR spectra of the adsorbed species at various temperatures in 6000 ppm NO and 2% O_2 on Cu^{2+}-Al-PILC. Compared to Fig. 2, these spectra, under in situ reaction conditions, indicate the significant intensity reduction at high temperatures.

Fig. 4 shows the spectra of Cu^{2+}-Al-PILC without exposure to NO and O_2. The spectrum at room temperature shows a broad band at 2900–3750 cm^{-1}, which was the stretching band for hydrogen bonded water adsorbed on the surface plus the hydroxyl groups. As the temperature was increased,

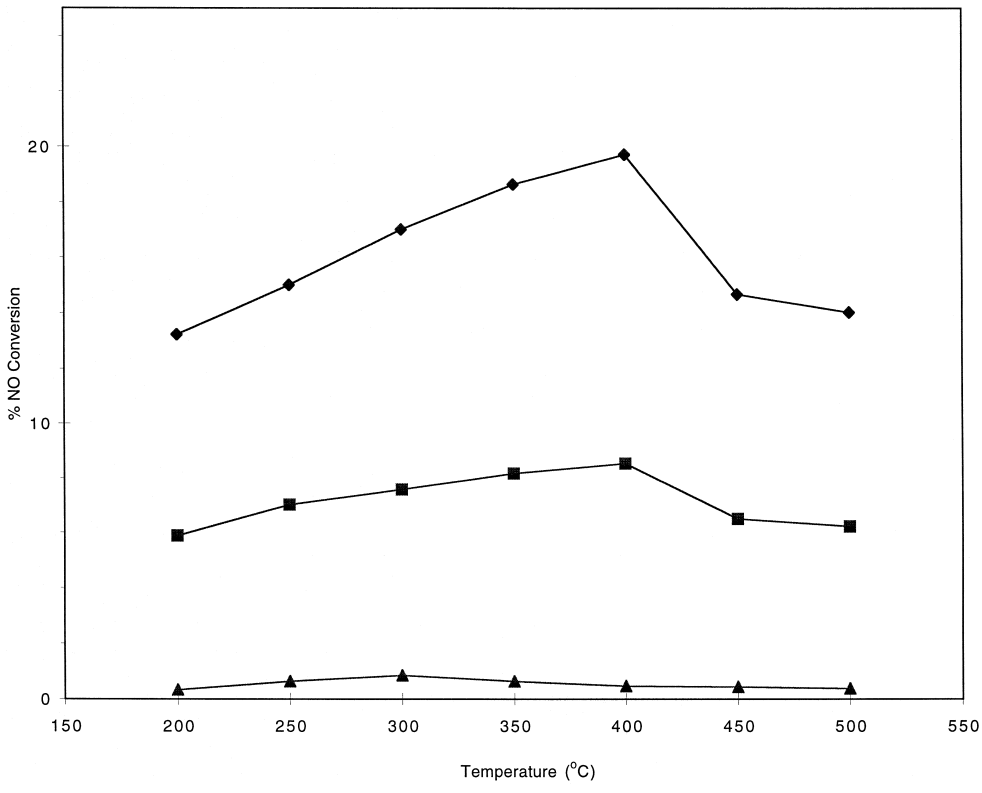

Fig. 5. Temperature dependence of NO decomposition on Cu-PILC at 4.0 g.s. cm^{-3} and $P_{NO} = 1\%$. Total NO conversion (♦), NO decomposition to N_2 (■) and NO decomposition to N_2O (▲).

water desorbed and this band became sharpened. Sharp bands at 3600–3750 cm^{-1} were due to free OH hydroxyl groups on the surface which could remain at temperatures substantially higher than 300°C.

3.2. Activities for NO decomposition

The activity of Cu^{2+}-Al-PILC for direct NO decomposition was measured and product analysis was made to obtain NO conversion and to obtain a complete product analysis of experiments was conducted at 4.0 g s cm^{-3} using 1% NO in He. The results for NO decomposition on Cu^{2+}-Al-PILC are given in Fig. 5. The results show small amounts of N_2O from NO decomposition. The N_2O concentration increased initially with temperature and subsequently leveled off. Except the peak position, its concentration history was parallel to that of N_2. The second series of experiments was conducted under the same conditions using Cu^{2+}-ZSM-5, and the activity results are shown in Fig. 6. A comparison of the SCR activity of NO with C_2H_4 between these two catalysts has already been made and will not be repeated here [31].

4. Discussion

Figs. 5 and 6 show respectively, the NO decomposition activities of the Cu-PILC and Cu-ZSM-5 catalysts. Complete product analyses (except for NO_2) were made, and mass balances for nitrogen

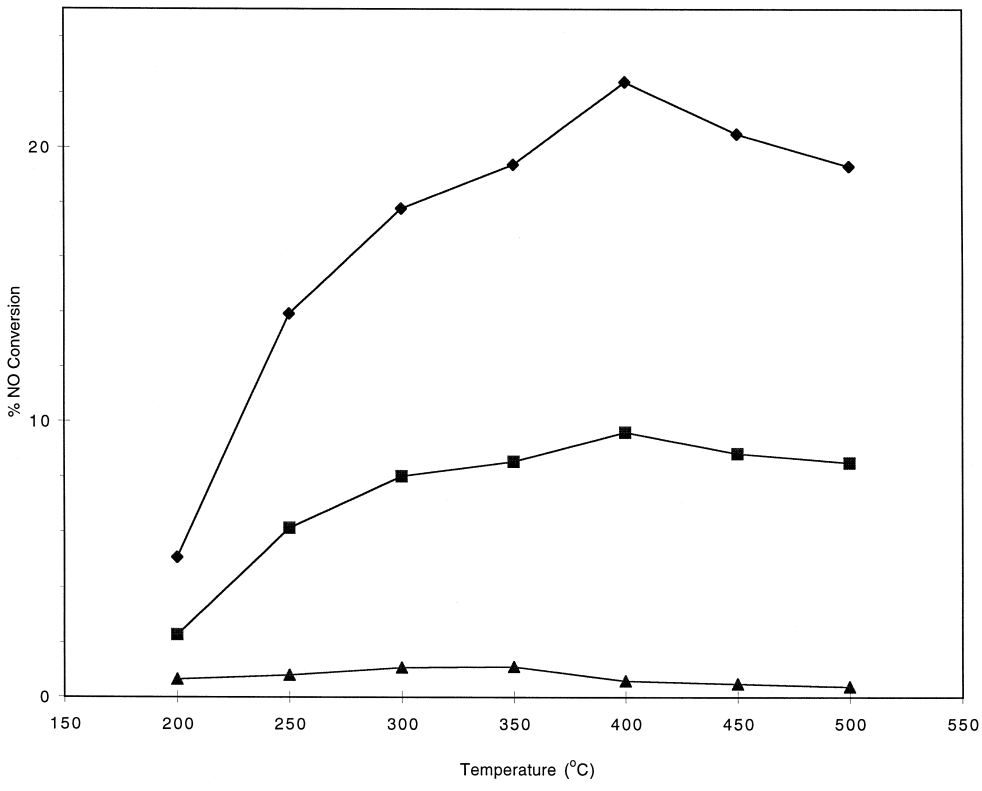

Fig. 6. Temperature dependence of NO decomposition on Cu-ZSM-5 at 4.0 g.s. cm^{-3} and $P_{NO} = 1\%$. Total NO conversion (♦), NO decomposition to N_2 (■) and NO decomposition to N_2O (▲).

were within 80–90% in all cases. The activity for Cu-PILC appeared to be lower than that of Cu-ZSM-5 at high temperatures (i.e., above 400°C) and higher at lower temperatures (i.e., below 300°C). The Cu^{2+} exchanges were 223% for Cu-ZSM-5 and 87.7% for Cu-PILC. Thus it is expected that the activity of Cu-PILC would have been higher than Cu-ZSM-5 if the % ion-exchange was the same [32,40]. Comparing the activity of Cu-ZSM-5 with the literature data, the activity was lower than that reported by Li and Hall [32]. This was due to the higher Si/Al ratio in our sample, i.e., [40] vs. [12].

In all NO decomposition experiments, small but significant amounts of N_2O were detected. The presence of N_2O provided an important piece of information to the understanding of the mechanism, as to be discussed shortly. The O_2 that was formed along with N_2 was reacted with NO to form NO_2 [32,40].

Owing to its stability at room temperature, the possibility of assigning the peak at 1699 cm^{-1} to physisorbed species is ruled out. This species is thought to be dinitrosyl, disappearing at temperatures greater than 100°C, and it was bonded to Cu^{+}. It was reported that both mononitrosyl and dinitrosyl species were formed on Cu^{+} sites, whereas mononitrosyl formed exclusively on Cu^{2+} ions [35,41,42]. The small shift from the band positions on Cu-ZSM-5 as assigned by Valyon and Hall (1827, 1734 cm^{-1}) [43] was possibly due to stronger coordination between the metal site on Cu-PILC and nitric oxide. The acceptance of an electron that is transferred from NO to a metal site is more favorable on Cu-PILC and thus, the bond strength of NO becomes weaker when compared to that on Cu-ZSM-5. The peak of symmetric stretching of dinitrosyl is not clearly shown. It might have been disguised by the broad band at 1699 cm^{-1}. Unlike the first peak, the shoulder at 1603 cm^{-1} demonstrated its thermal stability up to 300°C. It can be possibly assigned as NO_2-containing species (bands at 1630, 1608, 1574 and 1315 cm^{-1}) as in Refs. [37,42,44,45]. Nevertheless, due to its robustness which is not likely to be seen in nitro species, this species is more likely a nitrate species. Although the precise structures of these nitro and nitrate species are difficult to assign, many literature sources suggest that the structure is likely to be of the form bidentate nitrate [36,44,45]. The pair of bands at 1603 and 1300 cm^{-1} can be attributed to ν_3 split vibration of either bridged nitrate ($\Delta\nu_3 \approx 420$ cm^{-1}) or bidentate nitrate ($\Delta\nu_3 \approx 300$ cm^{-1}). However, $\Delta\nu_3$ of this species is closer to that of the bidentate nitrate. Also, a bridged nitrate would require two coupled sites to form, which is not a likely event. Therefore, this species is assigned to be bidentate. The bidentate ν_1 vibration frequency at 1040–1010 cm^{-1} could not be detected in this experiment. The remaining broad band is suspected to contain at least two species. They apparently split and drift apart at higher temperatures. The regions of 1440–1335 cm^{-1} and 1385–1250 cm^{-1} have been assigned to be $\nu_3(NO_2)$ ($\nu_3 = 1470$–1450 cm^{-1}) and $\nu_1(NO_2)$ ($\nu_1 = 1065$–1050 cm^{-1}) [44,45].

The NO_2 species has been attributed to be a key intermediate species for SCR on copper-on-alumina [46]. For ZSM-5, most of the surface species belong to either nitro species for Cu-ZSM-5 or nitrito for Co-ZSM-5 [47]. As the precise nature of the nitro, nitrito and nitrato species is not known, the bands in the region of 1530–1630 cm^{-1} and near 1300 cm^{-1} have been unspecifically assigned to all these species [43]. As a result, the active nitro species is assigned to be bidentate nitro or nitrito species. When the catalyst is further heated to 200°C, these two bands drift further apart to the new positions at 1571 and 1306 cm^{-1}. The peak positions at 1571 and 1306 cm^{-1} conform to that of the monodentate nitrate (NO_3^-) in the range of 1530–1480 cm^{-1} for ν_3(split) as noted in [44,45]. Its characteristic is consistent with that found by Bell and coworkers as the intensity grew from room temperature and then reduced at 300°C [36]. This assignment is plausible when comparing the monodentate nitrate with relatively low thermal stability and the adjacent peak of the bidentate nitrate [44].

From the spectra, two possible routes to form nitrate are suggested. One is formed directly from the dinitrosyl group, and the other is formed by reacting with the O–H groups. The first route can be explained as follows: At 100°C, the dinitrosyl species is unstable and rapidly decomposes to N_2O, while oxidizing the metal site to $Cu^{2+}O^-$. The N_2O species must be significantly active as it could not be detected by FTIR ($N_2O \sim 2220–2250\ cm^{-1}$). It is reported that N_2O decomposes to form N_2 on Cu-ZSM-5 more rapidly than NO because of its self-containing N_2 species which therefore requires only a single site [14]. The association of active monodentate nitrito or bidentate nitro (peak regions of 1440–1335 cm^{-1} and 1385–1250 cm^{-1}) with the available lattice oxygen eventually form monodentate nitrate (NO_3^-). The other possibility is seen from the noticeably negative O–H stretching peaks at near 3700 cm^{-1}. These negative bands are strong evidence that the nitro group, either from the gas phase or the adsorbed species, react with the hydroxyl group, thus forming nitrate, similar to that occurring on TiO_2 at 150°C [44]. ($2\ Cu–OH + 3\ NO_2 \rightarrow 2\ Cu–NO_3 + H_2O + NO$) The slightly negative peaks of O–H stretching at room temperature might be caused by the bidentate nitrate formation. The negative O–H stretching signal is attributed to the depletion of O–H bonds with Cu sites while water as a reaction product desorbs upon He purge or temperature increase. The increasing negative signal with temperature is due to more favorable condition for nitrate formation at higher temperatures. On the other hand, Bell and coworkers have proposed another route by having NO approaching Cu^{2+} sites instead, and subsequently forms a bidentate nitro species on Cu-ZSM-5 [36], and consequently generating N_2O_3 ($\sim 1600\ cm^{-1}$) via a Eley–Rideal type reaction between NO and the adsorbed bidentate nitrate [36,48]. However, the spectra in Fig. 1 clearly showed that there are no peaks of these species and thus, confirming that PILC has a different pathway to decompose NO. The proposed mechanism is summarized below.

5. Proposed mechanism

$$2Cu(OH)^+ \leftrightarrow 2Cu^+ + 1/2O_2 + H_2O \quad (1)$$

$$Cu^+ + 2NO \leftrightarrow Cu^+(NO)_2 \quad (2)$$

$$Cu^+(NO)_2 \leftrightarrow Cu^{2+}O^- + N_2O \quad (3)$$

$$Cu^{2+}O^- + N_2O \leftrightarrow Cu^+ + O_2 + N_2 \quad (4)$$

$$Cu^{2+}O^- + NO \leftrightarrow Cu^{2+}–O–N=O\ (\text{monodentate nitrito}) \quad (5a)$$

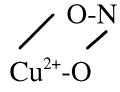

or (bidentate nitro) (5b)

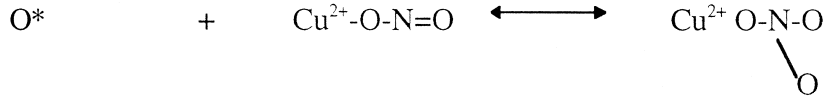

(6a)

where O* is lattice oxygen or extra lattice oxygen

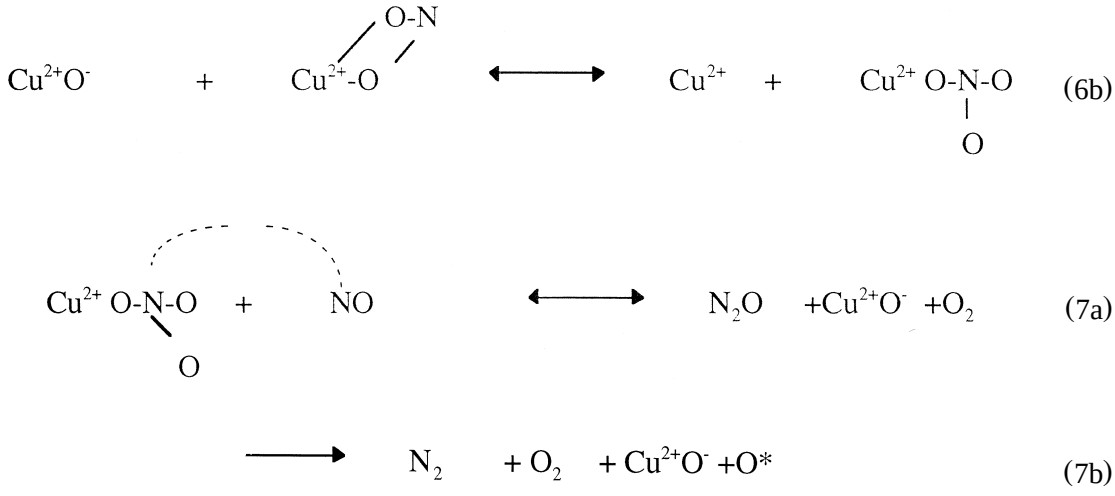

The above mechanism favors the redox cycle on the active sites. The initial occurrence of Cu^+ could be generated from slightly reduced conditions. Water molecules which are coordinated near Cu^{2+} ions are easily ionized and dissociated, and subsequently $Cu(OH)^+$ and Bronsted acid sites are formed as observed on Cu-MFI-116 zeolite [40]. Some lattice oxygen atoms are probably held by bridge structure of Cu^{2+}–O–Cu^{2+} from dehydroxylating the dimerization or polymerization of $CuOH^+$ on a fresh catalyst [43,40]. The appearance of Cu^+ is thus formed from the reduction of Cu^{2+} by $1/2\ O_2$ evolution [49]. The steps are summarized below, as in [50]:

$$2Cu(OH)^+ \rightarrow Cu^{2+}\text{–O–}Cu^{2+} + H_2O \quad \text{(i)}$$

$$Cu^{2+}\text{–O–}Cu^{2+} \rightarrow 2Cu^+ + 1/2O_2 \quad \text{(ii)}$$

Another possibility for Cu^+ formation is from the spontaneous desorption of O_2 [32]. Some cupric moieties migrate on the surface of the mesopores and thus the formation of a transient dicopper species generates cuprous ions through the desorption of O_2 [7,32]. Although O_2 coupling, especially in the bridge structure, which requires four cations, is quite rare as the metal sites are far apart, there is evidence for spontaneous oxygen desorption on Cu-zeolites even at low temperatures, e.g., room temperature [48]. The role of the Cu^+ species appears to be a trigger for the aforementioned mechanism. After the cycle is initiated, Cu^+ can be subsequently generated from other intermediates as shown in Eq. (4) through N_2O decomposition. The decomposition of NO to $N_2 + O_{ads}$ at elevated temperatures will lead to reoxidation of Cu^+ to Cu^{2+} and reduce back to Cu^+ under a steady supply of nitric oxide. This result is consistent with the findings of Iwamoto and Hamada [34] and of Li and Hall [32] and Hall and Valyon [33]. However, Shelef argued against the cyclic mechanism for NO decomposition. His observation was based on the requirement that the adsorption sites remain stable during reaction conditions and be resistant to chemisorption of oxygen [11]. He suggested gem–nitrosyl (two NO^- on one site) on Cu^{2+} as a key intermediate species for direct NO decomposition on Cu-ZSM-5. Further study by EPR of copper on PILC, both after adsorption and desorption of oxygen, seems desirable for elucidating the nature of these sites.

The role of N_2O is tentatively identified to be either as an initiator for the cyclic mechanism or a product from the parallel reactions [46]. Its instability and rapid direct decomposition over Cu-ZSM-5/Cu–Y zeolite [49] indicates that N_2O might be a key intermediate species for the direct NO

decomposition. Due to its paired-nitrogen structure, the decomposition of N_2O is a unimolecular reaction, in contrast to NO decomposition that requires pairing of two nitrogen-containing species. The GC results show the parallel concentration trend of N_2O with N_2 formation (Figs. 5 and 6). This result is in contrast to the cyclic mechanism in which N_2O forms initially during the formation of the active sites and then decreases [46]. For this reason, N_2O might be generated from the decomposition of another intermediate species which is proposed to be nitrate for Cu-PILC, while N_2O is thought to be generated from copper–nitrite–mononitrosyl for Cu-on-alumina catalyst [46]. However, the rate determining step for NO decomposition, following a Langmuir–Hinshelwood type mechanism, would require a surface reaction between two adsorbed NO molecules [51]. Therefore, the presence of intermediate N_2O enhances the overall NO conversion.

The rate limiting step for direct NO decomposition has long been described to be the nitrogen-pairing step. The conventional Langmuir–Hinshelwood model of pairing two adsorbed species yields the consistent result with the kinetic study of most transition metals on alumina and on quartz for direct NO decomposition [6]. However, the probability of pairing two adjacent sites is not high. Hence an Eley–Rideal type reaction between NO and a surface nitrite–mononitrosyl species (N_2O_3) has been proposed recently for Cu-ZSM-5 and Cu–alumina [31,36,52,50,51]. The result from our FTIR study clearly indicates that there are no adsorption bands due to Cu–N_2O_3 in the region of 1600 cm^{-1} for NO_2 bidentate and 1900 cm^{-1} for NO stretching as presented in [47,53]. As can be seen in Figs. 2 and 3, the decreased amount of monodentate nitrate from 200°C to 300°C under the reactant gases is much more appreciable in Fig. 3 than in Fig. 2. In the presence of O_2, the NO_3^- peak should have increased by oxidizing the nitro species. Thus, its decrease is possibly from reduction by NO in the gas phase, generating either N_2O or N_2 as shown in Eq. (7a). The N–N bond could not be detected in this experiment. This is possibly due to the short life of this intermediate species. However, Hierl et al. reported that nitrate simply decomposed back to NO and O_2 at higher temperatures from their thermodesorption study on CuO–Al_2O_3 [54]. Thus, a further study on the role of nitrate would shed light on this argument.

To study the effect of O_2, Fig. 2 has been recorded after adsorbing both NO and O_2 for half an hour. There are no new emerging peaks or any changes in intensities due to the addition of O_2. This observation clearly explains the role of the extra-lattice oxygen which could form the intermediate species without external O_2 supply. As can be seen when comparing Figs. 1 and 2, there is no significant influence from the additional O_2 when it is adsorbed at room temperature. Further product analysis needs to be made in order to determine any possible role of O_2. There is a possibility that for the fresh catalyst, the mechanism path follows Eq. (7b) rather than Eq. (7a). The total lattice oxygen is then preserved and thus adding the external oxygen supply has insignificant effect. When the catalyst is aged, an O_2 dose might help recover the activity; the mechanism path would shift to Eq. (7a) and consequently deplete the lattice oxygen. Eventually the external O_2 source is required to replenish the consumed amount. In contrast, the effect of supplying O_2 from external source or retaining O_2 from NO decomposition product can be negative if the active site is not selective for NO adsorption and reaction, as found on noble metal catalysts [55].

6. Conclusion

The activities for NO decomposition by Cu-PILC and Cu-ZSM-5 were similar. Product analysis showed small but significant amounts of N_2O with both catalysts. Based on in situ IR results and the product analysis, a reaction pathway for NO decomposition on Cu-PILC is proposed, which is

different from that on Cu-ZSM-5. The active intermediates under the reaction conditions are assigned to be nitro, nitrous oxide and nitrate. In this mechanism, N_2 can be generated from nitrate or nitrous oxide decomposition. It is likely that the reaction in Eq. (5b) occurs so rapidly that it is not possible to detect the short-life Cu–N_2O species by FTIR. However, the presence of a significant amount of N_2O in the gas phase provides support to the mechanism. From this study, it is clear that Cu–PILC contains a large reservoir of extra-lattice oxygen on a fresh catalyst. Consequently, adding the external O_2 supply has no significant effect. The proposed reaction is based on the cyclic redox mechanism of the Eley–Rideal type.

Acknowledgements

This work was supported by the US Department of Energy under Grant DE-FG22-96PC96206. We are grateful to Dr. Gordon Patterson of Laporte and Dr. N.V. Choudary of Indian Petrochemicals for the Laponite and ZSM-5 samples.

References

[1] K.C. Taylor, in Catalysis: Science and Technology, in: J.R. Anderson, M. Boudart (Eds.), Vol. 5, Springer, Berlin (1984).
[2] T.J. Truex, R.A. Searles, D.C. Sun, Platinum Metals Rev. 36 (1992) 2.
[3] J. Haggin, Pacifichem '95 Honolulu, C&E News, Am. Chem. Soc., Washington, DC, January 8, 1996.
[4] M. Iwamoto, N. Mizuno, J. Auto. Eng. 207 (1993) 23.
[5] G.P. Ansell, A.F. Diwell, S.E. Golunski, J.W. Hayes, R.R. Rajaram, T.J. Treux, A.P. Walker, Appl. Catal. B: Environ. 2 (1993) 81.
[6] J.W. Hightower, D.A. Van Leirburg, The Catalytic Chemistry of Nitrogen Oxides, in: R.L. Klimisch, J.G. Larson, (Eds.), Plenum, New York, 1975, pp. 63–94.
[7] D.J. Liu, H.J. Robota, Appl. Catal. B 4 (155) (1994) .
[8] M. Iwamoto, Symp. on Catalytic Technology for Removal of Nitrogen Oxides, Catal. Soc. Japan, 1990, pp. 17–22.
[9] W. Held, A. Konig, T. Richter, L. Puppe, SAE Paper 900469 (1990).
[10] C. Yokoyama, M. Mizuno, J. Catal. 150 (1994) 9.
[11] M. Shelef, Catal. Lett. 15 (1992) 305.
[12] M.D. Amiridis, T. Zhang, R.J. Farrauto, Appl. Catal. B 10 (1996) 203.
[13] B.K. Cho, J. Catal. 142 (1993) 418.
[14] J. Valyon, W.K. Hall, J. Catal. 143 (520) (1993) .
[15] J. Petunchi, G. Sill, W.K. Hall, Appl. Catal. B 2 (1993) 303.
[16] A.P. Ansell, A.F. Diwell, S.E. Colunski, J.W. Hayes, R.R. Rajaran, T.J. Truex, A.P. Walker, Appl. Catal. B 2 (1993) 101.
[17] C.H. Bartholomew, R. Gopalakrishnan, P.R. Stanford, J.E. Davison, W.C. Hecker, Appl. Catal. B 2 (1993) 183.
[18] Y. Li, J.N. Armor, Appl. Catal. B 3 (1992) L31.
[19] Z. Chajar, M. Primet, H. Praliaud, M. Chevrier, C. Gauthier, F. Mathis, Appl. Catal. B 4 (1994) 199.
[20] F. Witzel, G.A. Sill, W.K. Hall, J. Catal. 149 (1994) 229.
[21] Y. Li, J.N. Armor, J. Catal. 150 (1994) 376.
[22] Y. Li, T.L. Slaget, J.N. Armor, J. Catal. 150 (1994) 388.
[23] M. Misono, K. Kondo, Chem. Lett. 1001 (1991) .
[24] K.A. Bethke, D. Alt, M.C. Kung, Catal. Lett. 25 (1994) 37.
[25] M. Kung, K. Bethke, D. Alt, B. Yang, H. Kung, in: U.S. Ozkan, S. Agarwal, C. Marcelin (Eds.), NO_x Reduction, Chap. XX, ACS Symp. Ser., ACS Washington, DC, 1995.
[26] M.J. Heimrich, M.L. Deviney, SAE Paper 930 (1994) 736.
[27] D.R. Monroe, C.L. Dimaggio, D.D. Beck, F.A. Matekunas, SAE Paper SP 930737 (1994).
[28] J.N. Armor, Appl. Catal. B 4 (1994) N18.
[29] M. Shelef, Chem. Rev. 95 (1995) 209.
[30] R.T. Yang, W. Li, J. Catal. 155 (1995) 414.
[31] W. Li, M. Sirilumpen, R.T. Yang, Appl. Catal. B: Environ. 8 (1996) 372.
[32] Y. Li, W.K. Hall, J. Catal. 129 (1991) 202.
[33] W.K. Hall, J. Valyon, Catal. Lett. 15 (1992) 311.

[34] M. Iwamoto, H. Hamada, Catal. Today 10 (1991) 57.
[35] E. Giamello, D. Murphy, G. Magnacca, C. Morterra, Y. Shioya, T. Nomura, M. Anpo, J. Catal. 136 (1992) 510.
[36] A.W. Aylor, S.C. Larsen, J.A. Reimer, A.T. Bell, J. Catal. 157 (1995) 592.
[37] K. Hadjiivanov, D. Klissurski, G. Ramis, G. Busca, Appl. Catal. B 17 (251) (1996) .
[38] R.T. Yang, J.P. Chen, E.S. Kikkinides, L.S. Cheng, J.E. Cichanowicz, Ind. Eng. Chem. Res. 31 (1992) 144.
[39] Y. Li, J.N. Armor, Appl. Catal. B 5 (1995) 257.
[40] M. Iwamoto, H. Yashiro, K. Tanda, N. Mizuno, Y. Mine, S. Kagaw, J. Phys. Chem. 95 (1991) 3727.
[41] M. Iwamoto, H. Furukawa, S. Kagawa, Stud. Surf. Sci. Catal. 28 (1986) 943.
[42] G. Spoto, S. Bordiga, D. Scarano, A. Zecchina, Catal. Lett. 13 (1992) 39.
[43] J. Valyon, W.K. Hall, J. Phys. Chem. 97 (1993) 1204.
[44] K. Hadjiivanov, V. Busher, M. Kantcheva, D. Kliissurski, Langmuir 10 (1994) 464.
[45] A.A. Davydov, IR spectroscopy Applied to Surface Chemistry of Oxides; Nauka: Novosibirsk, 1984.
[46] G. Centi, S. Perathoner, J. Catal. 152 (1995) 93.
[47] B.J. Adelman, T. Bentel, G.-D. Lei, W.M.H. Sachtler, J. Catal. 158 (1996) 327.
[48] T. Cheung, S.K. Bhargava, M. Hobday, K. Goger, J. Catal. 158 (1996) 301.
[49] M. Iwamoto, K. Maruyama, N. Yamazoe, T. Seiyama, J. Phys. Chem. 81 (1987) 622.
[50] J.O. Petunchi, G. Marcelin, W.K. Hall, J. Phys. Chem. 96 (1992) 9967.
[51] M.A. Vannice, A.B. Walters, X. Chang, J. Catal. 159 (1996) 119.
[52] P.A. Jacobs, H.K. Beyer, J. Phys. Chem. 83 (1979) 1174.
[53] J. Szanyi, M.T. Paffett, J. Catal. 164 (1996) 232.
[54] R. Hierl, H.P. Urbach, H. Knozinger, J. Chem. Soc. Faraday Trans. 88 (3) (1992) 355.
[55] R. Burch, P.J. Millington, A.P. Walker, Appl. Catal. B 4 (1994) 65.